Longitudinal mode analysis of multisection ring and edge-emitting semiconductor lasers

Mindaugas Radziunas
Weierstrass Institute, Mohrenstrasse 39, 10117 Berlin, Germany. Email: Mindaugas.Radziunas@wias-berlin.de

***Abstract*—We present a method which allows computing and analyzing longitudinal optical modes in multisection ring and edge-emitting lasers, provided the traveling wave model gives an appropriate description for the dynamics in these devices.**

Multisection ring and edge-emitting semiconductor lasers (SL) are useful devices for different purposes. The small size and the high frequency of the optical field intensity modulation makes these devices interesting for optical data communications and their application in photonic integrated circuits. Modeling, simulations and analysis are crucial for optimizing of existing SLs as well as for designing new devices with a particular dynamical behavior.

We apply the software package `LDSL-tool` [1] for simulations and analysis of the SLs. This software allows considering a large variety of laser devices or coupled laser systems, which can be schematically represented by a set of mutually interconnected n_s *sections* and n_j *junctions*: see Fig. 1. According to the proposed laser device construction, for each front and rear edge z'_k and z''_k of any section $S_k = [z'_k, z''_k]$ one can attribute a unique junction. On the other hand, each junction J_l joins $j_l \geq 1$ section edges, so that $\sum_{l=1}^{n_j} j_l = 2n_s$.

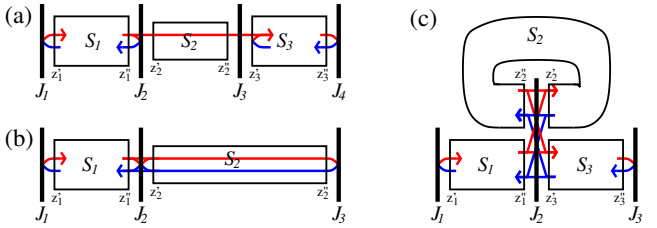

Fig. 1. Multisection lasers and coupled laser devices as sets of differently joined sections S_j and junctions J_l. (a): Master (S_1) – slave (S_3) laser system. (b): Laser (S_1) with an external feedback. (c): Ring laser (S_2) with a single outcoupling waveguide. In all cases, only a single longitudinal spatial dimension is taken into account.

Within each section we consider the spatial-temporal dynamics of the wave function $\Psi(z,t) = \binom{E}{p}$, where $E = \binom{E^+}{E^-}$ and $p = \binom{p^+}{p^-}$ denote complex slowly varying amplitudes of counter-propagating optical fields and polarizations, respectively. The dynamics of Ψ is governed by the field equations

$$-i\partial_t \Psi(z,t) = \mathcal{H}\left(\beta^{\pm}\right)\Psi + \mathcal{F}_{sp}, \quad z \in S_k, \ k = 1,\dots,n_s, \quad (1)$$

where operator $\mathcal{H}$ is defined by a 4×4 matrix

$$\mathcal{H}(\beta^{\pm}) = \begin{pmatrix} v_g H_0(\beta^{\pm}) + \frac{iv_g\bar{g}}{2}\mathcal{I} & -\frac{iv_g\bar{g}}{2}\mathcal{I} \\ -i\bar{\gamma}\mathcal{I} & (i\bar{\gamma}+\bar{\omega})\mathcal{I} \end{pmatrix},$$

$$H_0(\beta^{\pm}) = \begin{pmatrix} i\partial_z - \beta^+ & -\kappa^- \\ -\kappa^+ & -i\partial_z - \beta^- \end{pmatrix}, \quad \mathcal{I} = \begin{pmatrix} 1 & 0 \\ 0 & 1 \end{pmatrix}.$$

$\beta^{\pm}(z,t)$ in the expressions above represents the complex propagation factors of the optical fields. In the passive parts of the laser, these factors are just complex constants determining scattering losses and possible additional rotation of the field functions. In the active part of the device, they depend on the dynamically changing carriers. When considering quantum-well [2] or quantum-dot SLs [3], one can use different models for $\beta^{\pm}$ and corresponding carrier dynamics. It is noteworthy, that, in contrast to linear laser configurations, the difference $\Delta_\beta = \beta^+ - \beta^-$ in ring SLs is, in general, non-vanishing [4].

To close the TW model (1), one should define all fields E^+ and E^- *incoming* into all sections of the SL. These fields are determined by the field reflection and transmission conditions

$$\mathcal{E}_l^i = \mathcal{T}_l \mathcal{E}_l^o, \quad l = 1,\dots,n_j. \quad (2)$$

Here, the vector $\mathcal{E}_l^i$, which denotes the required fields *incoming* into all j_l section edges attached to the junction J_l, is related to the vector $\mathcal{E}_l^o$ defining all fields *outgoing* from those edges.

$\mathcal{T}_l$ in the expression above is the $j_l \times j_l$-dimensional complex valued matrix denoting the field scattering at the junction J_l. For the junction of two adjacent sections in the linear device ($j_l = 2$) it is usually given by the simple identity matrix, $\mathcal{I}$. At the junctions corresponding to the laser facets ($j_l = 1$) it determines the field reflection and is given by a complex constant r_l, $|r_l| \leq 1$. For the junction corresponding to the coupling between the ring laser and the linear waveguide (J_2 in Fig. 1(c)) it can be given as

$$\mathcal{T}_2 = \begin{pmatrix} T_2 & i\tilde{T}_2 & -r_2^* & 0 \\ i\tilde{T}_2 & T_2 & 0 & 0 \\ r_2 & 0 & T_2 & i\tilde{T}_2 \\ 0 & 0 & i\tilde{T}_2 & T_2 \end{pmatrix}, \quad T_2^2 + \tilde{T}_2^2 + |r_2|^2 \leq 1,$$

where T_2 and $\tilde{T}_2$ are the field transmission coefficients to the ahead and aside located sections, whereas r_2 models small localized back-reflection of the optical field [4]. In the general case, the coefficients of the matrices $\mathcal{T}_l$ can be frequency-dependent, and their estimation can require appropriate measurements or an advanced modeling, which takes into account the curvature of the adjacent sections, the field diffraction, and the overlapping of the lateral modes in the coupling region.

The concept of optical modes plays a significant role for understanding laser dynamics in general. They represent the natural oscillations of the electromagnetic field and determine the optical frequency and the life time of the photons contained in the given laser cavity. The *instantaneous* optical modes of linear multisection lasers were discussed, e.g., in Ref. [5]. These modes are pairs $(\Omega(\beta^{\pm}), \Theta(z,\beta^{\pm}))$ of eigenvalues and eigenvectors of the spectral problem

$$\Omega\Theta(z,t) = \mathcal{H}\left(\beta^{\pm}\right)\Theta(z,t), \quad z \in S_k, \ k = 1,\dots,n_s, \quad (3)$$

978-1-4799-3682-3/14/$31.00 ©2014 IEEE

which satisfies the boundary conditions (2) and is determined at *instantaneous* distributions of $\beta^{\pm}(z,t)$. The imaginary and the real parts of the complex eigenvalues Ω are mainly determining the angular frequency and the damping of the corresponding mode. Thus, eigenvectors $\Theta(z,\beta^{\pm})$ of modes with vanishing $\Im m\,\Omega$ are defining (stable or unstable) stationary (continuous wave) states with optical frequencies $\Re e\,\Omega$.

In the previous work [5], the methods for computation of instantaneous modes in linear SLs were discussed. It appears, that similar algorithms also apply for the general case. Namely, the Eqs. (3) in each section S_k can be rewritten as two linear ODEs for optical field mode components $\Theta_E^{+}(z,\beta^{\pm})$ and $\Theta_E^{-}(z,\beta^{\pm})$, which can be solved by means of 2×2-dimensional transfer matrices,

$$\begin{pmatrix}\Theta_E^{+}\\ \Theta_E^{-}\end{pmatrix}(z_k'',\beta^{\pm}) = \mathcal{M}(\Omega,\beta^{\pm})\begin{pmatrix}\Theta_E^{+}\\ \Theta_E^{-}\end{pmatrix}(z_k',\beta^{\pm}),\quad k=1,\ldots,n_s.$$

Together with the reflection-transmission conditions (2), the relations above are providing $4n_s$ linear equations for $4n_s$ mode functions $\Theta_E^{\pm}$ at the section edges z_k' and z_k''. The determinant of this system of linear equations, $\chi(\Omega,\beta^{\pm})$, is a complex-valued function depending on the propagation factors $\beta^{\pm}$ and complex frequency Ω. Once the function $\chi(\Omega)\not\equiv 0$, the set of its roots coincide with a set of all complex mode frequencies.

Two examples below illustrate the usefulness of the mode analysis in explaining the dynamical behavior of the SLs.

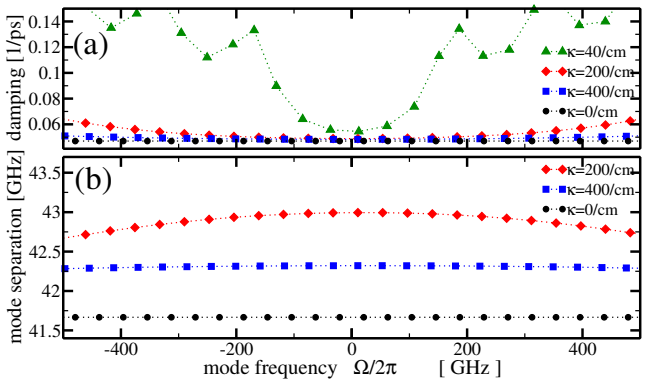

Fig. 2. Calculated mode damping $\Im m(\Omega_k)$ (top) and frequency separation $\Re e(\Omega_k-\Omega_{k-1})$ of the adjacent modes (bottom) vs. mode frequency $\Im m(\Omega_k)$ for the Fabry-Perot laser and the lasers with different DBR.

In the first example, single section Quantum Dash based self mode-locked (ML) SLs with integrated passive distributed Bragg reflectors (DBR) were considered [6]. In all cases, the total length of the SL was 1 mm, whereas $\kappa L_{BG}=1$. The length of the DBR part of the laser, L_{BG}, was chosen to be 250, 50 or 25 μm. The measurements have shown that the laser with $L_{BG}=25\,\mu$m and $\kappa=400\,\mathrm{cm}^{-1}$ could emit the self-ML pulses comparable to those observed in a single-section Fabry-Perot quantum dash laser. While the ML pulsations in SL with $L_{BG}=50\,\mu$m and $\kappa=200\,\mathrm{cm}^{-1}$ had a rather large radio-frequency linewidth, the SL with $L_{BG}=250\,\mu$m and $\kappa=40\,\mathrm{cm}^{-1}$ was not suitable for ML at all. Fig. 2 presents the mode analysis of such devices. The upper diagram shows, how the introduction of the grating changes the relative positions of the complex mode frequencies Ω. For $\kappa=40\,\mathrm{cm}^{-1}$ only a few modes located within the ~ 300 GHz wide stop-band have similar thresholds, whereas the damping of all other modes is large. A typical performance of such DBR laser is the cw operation at the maximal gain mode, or the mode-beating type pulsations involving a couple of modes. In the cases of $\kappa=200\,\mathrm{cm}^{-1}$ and $\kappa=400\,\mathrm{cm}^{-1}$, the damping of 20 or even more modes within the stop-band is not much different. However, for a smaller κ, the DBR violates significantly the equidistance of the mode frequencies (panel (b)), which is equally important for the realization of ML pulsations.

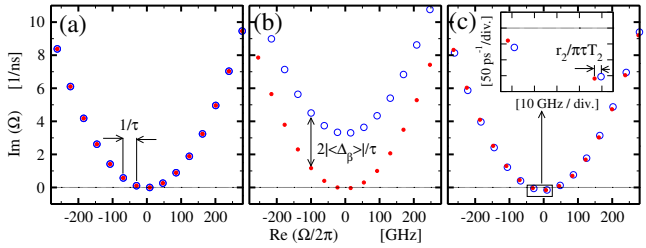

Fig. 3. Mode frequencies Ω of the ring SL for $\kappa^{\pm}=r_2=\langle\delta_\beta\rangle=0$ (a), $\kappa^{\pm}=r_2=0$ but $\langle\Delta_\beta\rangle\neq 0$ (b), and $\kappa^{\pm}=\langle\Delta_\beta\rangle=0$ but $r_2=0.2$ (c).

Fig. 3 represents another example of the mode analysis. A study of the complex function $\chi(\Omega,\beta^{\pm})$ suggests the appearance of the complex frequencies Ω in pairs, whereas, for small or vanishing $\kappa^{\pm}$, the adjacent pairs are separated by the field round-trip frequency τ^{-1}. In the degenerate case, when backscattering r_2 or $\kappa^{\pm}$ and spatially averaged difference $\langle\Delta_\beta\rangle$ vanish, the mode frequencies within each pair coincide: see Fig. 3(a). In this case, the simulations show multiple stable cw states with different contributions of counter-propagating fields operating at the same frequency. Once the degeneracy disappears, the mode pairs split, resulting in different dynamical regimes of the ring SL. For example, Fig. 3(b) and (c) show the mode splitting corresponding to the unidirectional cw state and over-modulated alternating oscillations, respectively.

In conclusion, the computation of the optical modes leads to a better understanding of the nonlinear dynamics of semiconductor laser devices and is very useful when optimizing existing semiconductor lasers or designing new devices with a particular dynamical behavior.

Acknowledgment

The author would like to thank the support of EU FP7 ITN PROPHET, Grant No. 264687.

References

[1] LDSL-tool: a software package for simulation and analysis of longitudinal dynamics in semiconductor lasers. http://www.wias-berlin.de/software/ldsl/

[2] U. Bandelow, M. Radziunas, J. Sieber, and M. Wolfrum, *IEEE J. Quantum Electron.*, **37**, pp. 183–188, 2001.

[3] M. Radziunas, A. Vladimirov, E. Viktorov, G. Fiol, H. Schmeckebier, and D. Bimberg, *Appl. Phys. Lett.*, **98**, p. 031104, 2011.

[4] M. Radziunas, in *SPIE Proceedings Series*, **6997**, 2008, p. 69971B.

[5] M. Radziunas and H.-J. Wünsche, in *Optoelectronic Devices - Advanced Simulation and Analysis*, J. Piprek, Ed. Springer, 2005, pp. 121–150.

[6] S. Joshi, C. Calò, N. Chimot, M. Radziunas, R. Arkhipov, S. Barbet, A. Accard, A. Ramdane, and F. Lelarge, 2014, submitted.